Dengue-specific CD8+ T cell subsets display specialized transcriptomic and TCR profiles

Yuan Tian, … , Bjoern Peters, Alessandro Sette

Research Article **Immunology** **Infectious disease**

Accumulating evidence demonstrates that CD8+ T cells contribute to protection from severe dengue virus (DENV) disease and vaccine efficacy. Nevertheless, molecular programs associated with DENV-specific CD8+ T cell subsets have not been defined. Here, we studied the transcriptomic profiles of human DENV-specific CD8+ T cells isolated after stimulation with DENV epitopes from donors who had been infected with DENV multiple times and would therefore be expected to have significant levels of adaptive immunity. We found that DENV-specific CD8+ T cells mainly consisted of effector memory subsets, namely CD45RA−CCR7− effector memory (Tem) and CD45RA+CCR7− effector memory re-expressing CD45RA (Temra) cells, which enacted specific gene expression profiles upon stimulation with cognate antigens. DENV-specific CD8+ T cell subsets in general, and Temra cells in particular, were fully activated and polyfunctional, yet associated with relatively narrow transcriptional responses. Furthermore, we found that DENV-specific CD8+ Tem and Temra cells showed some unique T cell receptor features in terms of overlap and variable (V) gene usage. This study provides a transcriptomic definition of DENV-specific activated human CD8+ T cell subsets and defines a benchmark profile that vaccine-specific responses could aim to reproduce.

Find the latest version:

https://jci.me/123726/pdf

Dengue-specific CD8+ T cell subsets display specialized transcriptomic and TCR profiles

Yuan Tian,[1] Mariana Babor,[1] Jerome Lane,[1] Grégory Seumois,[1] Shu Liang,[1] N.D. Suraj Goonawardhana,[2] Aruna D. De Silva,[1,2] Elizabeth J. Phillips,[3,4] Simon A. Mallal,[3,4] Ricardo da Silva Antunes,[1] Alba Grifoni,[1] Pandurangan Vijayanand,[1] Daniela Weiskopf,[1] Bjoern Peters,[1,5] and Alessandro Sette[1,5]

[1]Division of Vaccine Discovery, La Jolla Institute for Immunology, La Jolla, California, USA. [2]Department of Paraclinical Sciences, General Sir John Kotelawala Defense University, Ratmalana, Sri Lanka. [3]Department of Medicine, Vanderbilt University Medical Center, Nashville, Tennessee, USA. [4]Institute for Immunology and Infectious Diseases, Murdoch University, Murdoch, Western Australia, Australia. [5]Department of Medicine, UCSD, La Jolla, California, USA.

Accumulating evidence demonstrates that CD8+ T cells contribute to protection from severe dengue virus (DENV) disease and vaccine efficacy. Nevertheless, molecular programs associated with DENV-specific CD8+ T cell subsets have not been defined. Here, we studied the transcriptomic profiles of human DENV-specific CD8+ T cells isolated after stimulation with DENV epitopes from donors who had been infected with DENV multiple times and would therefore be expected to have significant levels of adaptive immunity. We found that DENV-specific CD8+ T cells mainly consisted of effector memory subsets, namely CD45RA−CCR7− effector memory (Tem) and CD45RA+CCR7− effector memory re-expressing CD45RA (Temra) cells, which enacted specific gene expression profiles upon stimulation with cognate antigens. DENV-specific CD8+ T cell subsets in general, and Temra cells in particular, were fully activated and polyfunctional, yet associated with relatively narrow transcriptional responses. Furthermore, we found that DENV-specific CD8+ Tem and Temra cells showed some unique T cell receptor features in terms of overlap and variable (V) gene usage. This study provides a transcriptomic definition of DENV-specific activated human CD8+ T cell subsets and defines a benchmark profile that vaccine-specific responses could aim to reproduce.

Introduction

Dengue virus (DENV) infection is a serious public health problem in tropical and subtropical areas, and it is estimated that approximately 390 million people are infected yearly (1). DENV infection is associated with a range of clinical manifestations, from asymptomatic to life-threatening. More severe dengue disease presentations including dengue hemorrhagic fever and dengue shock syndrome are usually associated with heterotypic secondary infections with one of the four different serotypes (DENV1–DENV4) (2), which is postulated to be at least partially mediated by non-neutralizing serotype cross-reactive antibodies that can lead to antibody-dependent enhancement of infection (3–5).

The role of CD8+ T cells in dengue infection has been the subject of intense debate. Although some initial studies postulated that T cells may exacerbate the development of dengue diseases, subsequent studies indicate that T cells may have protective functions (6–8). CD8+ T cells have been shown to mediate protection in murine models of DENV infection and vaccination (9–12), and CD8+ T cells can confer protection against heterotypic DENV infection and prevent antibody-dependent enhancement (13–15). In humans, DENV-specific CD8+ T cells can migrate to the skin,

and their frequency may be inversely correlated with disease severity (16, 17). Notably, high-magnitude and polyfunctional DENV-specific CD8+ T cell responses are associated with protective HLA alleles against severe dengue disease in the general populations of Sri Lanka and Nicaragua, where DENV infection is highly endemic (18, 19). The recently approved Dengvaxia vaccine was designed to induce humoral but not CD8+ T cell responses against DENV. However, its suboptimal efficacy, coupled with safety adverse events, signals that the need for an efficacious DENV vaccine is still unmet. Most importantly, these issues urge a better understanding of DENV-specific CD8+ T cell responses at the cellular and molecular levels.

Surprisingly, the phenotypic and transcriptomic profiles of isolated human DENV-specific CD8+ T cell subsets have not yet been systematically interrogated. Some information exists related to the transcriptional signatures of whole blood and PBMCs in DENV-infected patients (23–26); however, much less is known at the level of human T cells. Although transcriptomic analyses of human CD8+ T cells from DENV-infected patients have been conducted, in those studies the gene expression profiles were analyzed not at the level of antigen-specific CD8+ T cells, but at the level of activated CD8+ T cell populations (27). Furthermore, little information exists at the level of CD8+ T cell subsets, such as Tcm, Tem, and Temra cells. This is particularly relevant as CD8+ Temra cells have been implicated in protection from viral pathogens such as HIV, cytomegalovirus (CMV), Epstein-Barr virus (EBV), influenza virus, and yellow fever virus in humans (28–32). Thus, it is

possible that some unique molecular profiles might be associated with CD8+ Temra cells that are virus-specific and activated by cognate antigens. Indeed, previous studies have compared the gene expression profiles and phenotypic attributes of human CD4+ T cell subsets and identified unique characteristics of CD4+ Temra cells (33, 34). A subset of CD4+ Temra cells has a highly specialized gene expression program and acquires the expression of cytotoxic molecules (33, 34), highlighting the general concept that T cell differentiation can result in downregulation of "irrelevant" programs and/or acquisition of new or enriched gene expression programs. However, whether the differentiation of CD8+ Temra cells also results in similar gene expression patterns is not known.

In this study, we isolated and systematically characterized the immune signatures of DENV-specific CD8+ T cell subsets after stimulation with DENV epitopes. Our data show that DENV-specific CD8+ T cells predominantly consist of Tem and Temra cells, which upregulated the expression of gene modules associated with activation, costimulation, and effector functions. The gene expression patterns of DENV-specific CD8+ T cells, especially Temra cells, are associated with relatively narrow transcriptional responses, suggesting that the differentiation of antigen-specific CD8+ T cell subsets is associated with a focused and specialized approach.

Results

DENV-specific CD8+ T cells are predominantly Tem and Temra. To investigate the phenotypic and functional characteristics of DENV-specific CD8+ T cells, we focused on cells identified by the production of IFN-γ after stimulation with a previously defined pool of over 268 CD8 DENV epitopes (35), which allows for broad coverage of DENV responses, irrespective of HLA type and DENV serotype, and is referred to hereafter as the DENV megapool (CD8 MP). This strategy was put in place based on previous observations that indicated that the majority of DENV-specific CD8+ T cells are strong producers of IFN-γ and thus could be detected ex vivo (19).

A series of previous studies from our group characterized DENV-specific CD8+ T cell responses in the context of natural immunity in populations heavily exposed to DENV (18, 19, 35). Here, following a similar approach, plasma samples from normal blood donors from the general hyperendemic population of the Colombo region in Sri Lanka were screened for high neutralizing titers against multiple DENV serotype, reflective of previous multiple DENV infections. PBMCs from donors that had been infected with DENV multiple times were stimulated with the DENV megapool, and the memory phenotype of these DENV-specific CD8+ T cells was determined by the expression of the commonly used memory markers CD45RA and CCR7. Gating strategies and FACS profiles for a representative donor are shown in Figure 1A.

In a total of 6 donors analyzed, the frequency of IFN-γ+ CD8+ T cells ranged from 0.05% to 5.19% with a median value of 0.36% after unstimulated control responses were subtracted (Figure 1B). This relatively wide range is consistent with previous results (35), and might reflect variations in the previous infection history and time from infection, which is unknown for the blood bank donors analyzed in this study. While a prominent naive T (Tn) cell population was readily detectable among unstimulated IFN-γ− CD8+

T cells, the vast majority of IFN-γ+ CD8+ T cells in the DENV megapool–stimulated group displayed either a CD45RA−CCR7− effector memory T (Tem) or a CD45RA+CCR7− effector memory T re-expressing CD45RA (Temra) phenotype (Figure 1C), also consistent with a previous report (19). To further confirm the Tem and Temra phenotype of DENV-specific CD8+ T cells without peptide stimulation, we used a previously defined pool of eight HLA-B*35:01 tetramers incorporating 8 different HLA-B*35:01–restricted DENV epitopes (19). Consistent with the phenotype of DENV IFN-γ+ cells, the majority of HLA-B*35:01 tetramer–positive CD8+ T cells displayed a Tem or Temra phenotype (Supplemental Figure 1; supplemental material available online with this article; https://doi.org/10.1172/JCI123726DS1) in tested HLA-matched donors. Thus, these results demonstrate that the frequency of anti-DENV CD8+ T cells varies between individuals, and that DENV-specific CD8+ T cells are primarily composed of Tem and Temra cells.

Gene expression profiles of unstimulated and DENV IFN-γ+ CD8+ Tem and Temra cells. Since DENV-specific CD8+ T cells were predominantly Tem and Temra cells as shown in Figure 1, we next isolated DENV IFN-γ+ CD8+ Tem and Temra cells and studied their immune signatures by bulk RNA sequencing (RNA-Seq). As a control, we also performed RNA-Seq on sorted IFN-γ− CD8+ Tem and Temra cells from unstimulated PBMCs. We then performed principal component analysis to visualize the global gene expression patterns of these various CD8+ T cell subsets. As expected, unstimulated CD8+ Tem and Temra cells were separated and formed distinct clusters. In contrast, DENV IFN-γ+ CD8+ Tem and Temra cells were grouped together, forming a distinct cluster that was well separated from unstimulated CD8+ Tem and Temra cells (Figure 2A). Thus, the gene expression signatures of DENV IFN-γ+ CD8+ Tem and Temra cells are clearly different from those of their unstimulated counterparts.

Next, we performed pairwise analyses to identify differentially expressed (DE) genes between the different sorted T cell subsets, namely stimulated DENV IFN-γ+ versus unstimulated Tem cells (Figure 2B), stimulated DENV IFN-γ+ versus unstimulated Temra cells (Figure 2C), unstimulated Tem versus Temra cells (Figure 2D), and stimulated DENV IFN-γ+ Tem versus Temra cells (Figure 2E). DE genes that resulted from these comparisons can be found in Supplemental Table 2. As expected, *IFNG* and many genes associated with activation and effector functions, such as *CD69*, *CD160*, *CRTAM*, *SLAMF7*, *TNFRSF9*, *TNF*, *CCL3*, *CCL4*, and *GZMB*, were upregulated in both DENV IFN-γ+ Tem and Temra cells (Figure 2, B and C, and Supplemental Table 2). Additionally, the expression of several costimulatory molecules, such as *CTLA4* and *TNFSF14*, as well as transcription factors such as *EGR1*, *EGR2*, *EGR3*, *IRF4*, and *IRF8* was also increased in DENV IFN-γ+ Tem and Temra cells (Figure 2, B and C, and Supplemental Table 2). Since CD8 MP–stimulated IFN-γ− CD8+ T cell subsets were exposed to the DENV-derived epitopes similarly but did not respond to stimulation, they could serve as another transcriptomic baseline in addition to unstimulated CD8+ T cell subsets. Therefore, we analyzed the DE genes between stimulated DENV IFN-γ+ versus stimulated IFN-γ− Tem cells as well as stimulated DENV IFN-γ+ versus stimulated IFN-γ− Temra cells. Using this approach, 515 and 767 DE genes were identified by Tem and Temra comparisons, respectively (Sup-
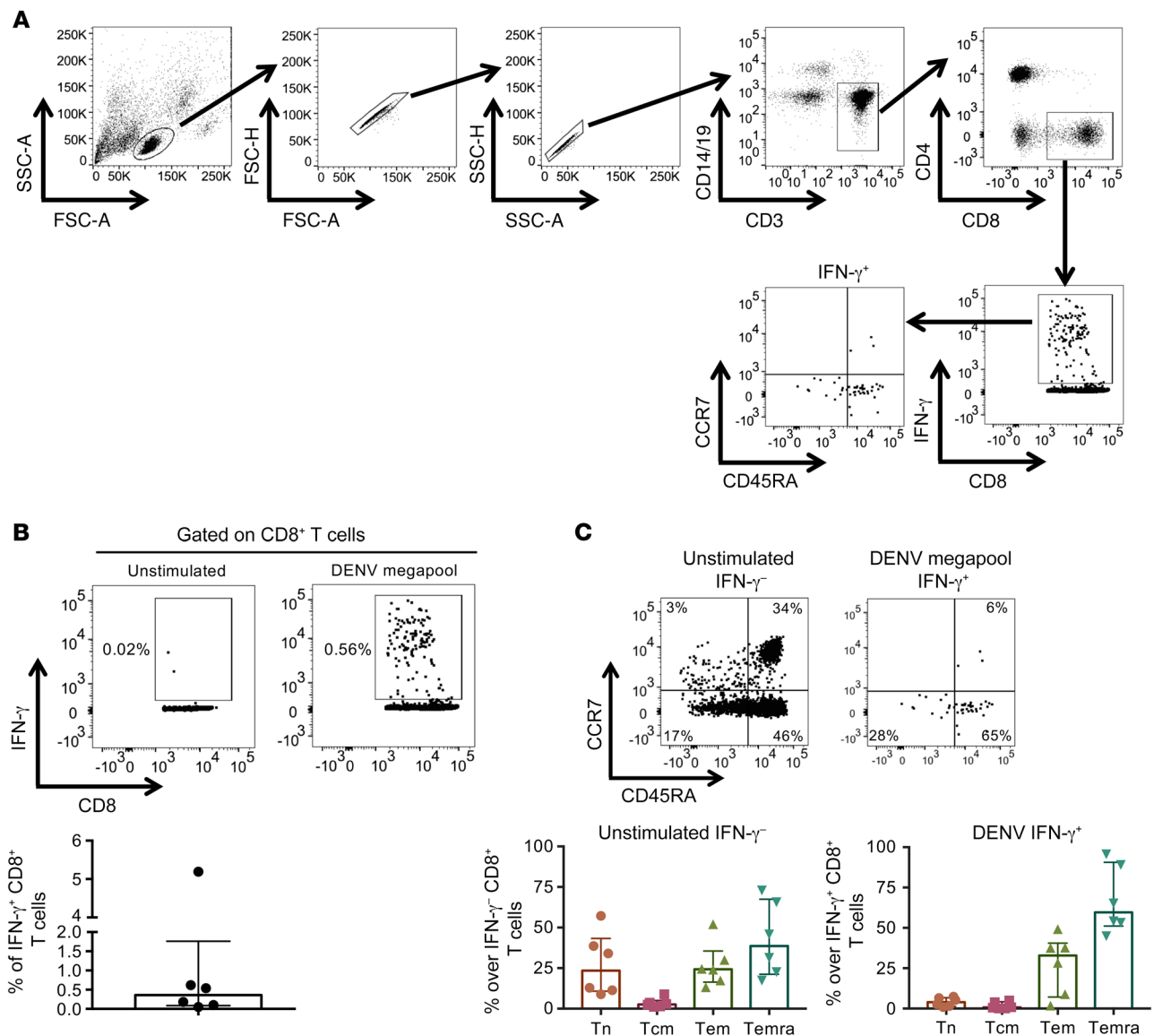
Figure 1. DENV-specific CD8+ T cells are predominantly Tem and Temra cells. Human PBMCs isolated from donors that had been infected with DENV multiple times were stimulated with DENV CD8+ T cell megapool, and DENV-specific CD8+ T cells were identified by the production of IFN-γ. (**A**) Gating strategy to identify and sort DENV-specific CD8+ Tem and Temra cells. (**B**) Flow cytometry plots (top) and bar graph (bottom) show the production of IFN-γ by CD8+ T cells (*n* = 6). (**C**) Flow cytometry plots (top) and bar graphs (bottom) show the expression of CD45RA and CCR7 by unstimulated IFN-γ⁻ or DENV IFN-γ⁺ CD8+ T cells (*n* = 6). Error bars show median with interquartile range.

plemental Figure 2, A and B). Notably, over 52% (270 genes) of the Tem DE genes and 60% (464 genes) of the Temra DE genes were also detected by stimulated DENV IFN-γ⁺ versus unstimulated comparisons presented in Figure 2, B and C, and Supplemental Table 2 (Supplemental Figure 2, A and B). Moreover, the overlapping genes include genes such as *IFNG*, *CD69*, *CRTAM*, *SLAMF7*, *TNFRSF9*, *TNF*, *CCL3*, *CCL4*, *GZMB*, *CTLA4*, *EGR1*, *EGR2*, *EGR3*, *IRF4*, and *IRF8* as described above (Supplemental Figure 2, C and D, and Supplemental Table 3). Moreover, the fold changes of these overlapping genes were highly correlated between these two approaches (Supplemental Figure 2, C and D).

We next identified differentially expressed genes between unstimulated Tem and unstimulated Temra cells and found that Temra cells had enhanced expression of the transcription fac-

tor *ZEB2* and several killer cell immunoglobulin-like receptors (KIRs), including inhibitory *KIR2DL1*, *KIR2DL3*, *KIR3DL1*, and *KIR3DL2* and activating *KIR2DS4* (Figure 2D and Supplemental Table 2), which bind to HLA-C2, HLA-C1, HLA-A/B with Bw4 epitope, HLA-A, and HLA-C/A, respectively (36). This suggests that CD8+ Temra cells may resemble natural killer (NK) cells and have more specialized cytotoxic functions than Tem cells. Moreover, although the number of differentially expressed KIRs was reduced, the expression level of *KIR2DL3* and *KIR3DL1* was also higher in DENV IFN-γ⁺ Temra by comparison with DENV IFN-γ⁺ Tem cells (Figure 2E and Supplemental Table 2). Interestingly, Tem cells had approximately 2.5-fold more upregulated genes by comparison with Temra cells (215 vs. 85 genes; Figure 2D), suggesting that CD8+ Temra cells have a more focused gene expression pattern
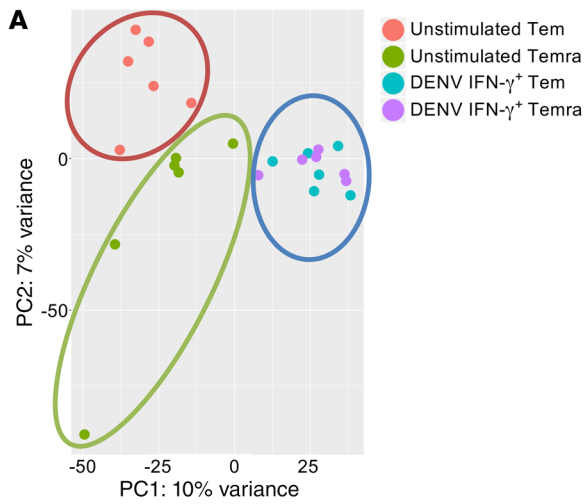
Figure 2. Gene expression profiles of unstimulated and DENV IFN-γ+ CD8+ Tem and Temra cells. (**A**) PCA analysis of gene expression data of unstimulated and DENV IFN-γ+ CD8+ Tem and Temra cells (*n* = 6). (**B**–**E**) Volcano plots show log$_2$ fold change versus –log$_{10}$ adjusted *P* value (*P*adj) for the comparison between DENV IFN-γ+ Tem and unstimulated Tem (**B**), DENV IFN-γ+ Temra and unstimulated Temra (**C**), unstimulated Tem and unstimulated Temra (**D**), and DENV IFN-γ+ Tem and DENV IFN-γ+ Temra (**E**). The subset of genes with log$_2$ fold change greater than 1 or less than –1 and adjusted *P* value less than 0.05 are considered significant and indicated by dotted lines. (**F**) Venn diagrams show the distribution of the 85 and 104 genes upregulated in unstimulated Temra and DENV IFN-γ+ Temra by comparison with unstimulated Tem and DENV IFN-γ+ Tem cells, respectively, as shown in **D** and **E**.
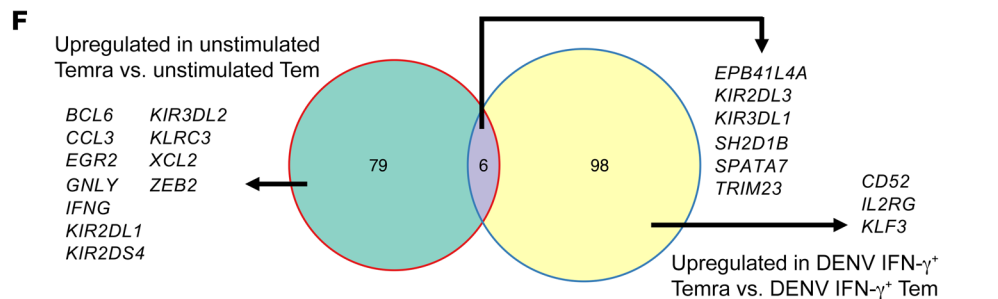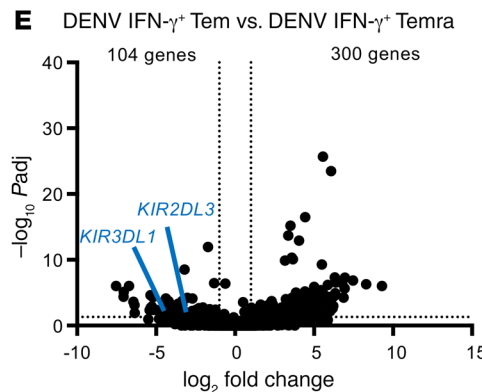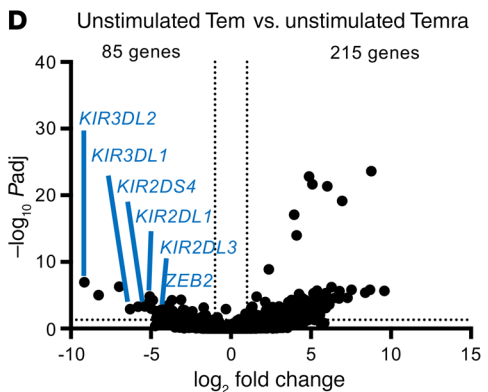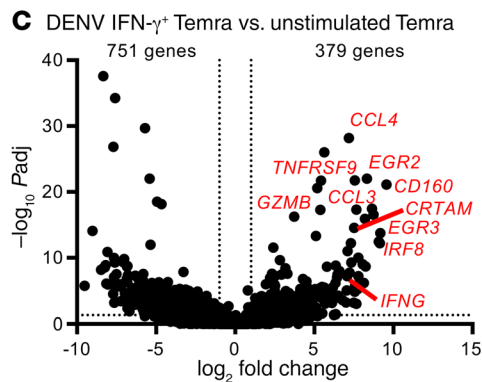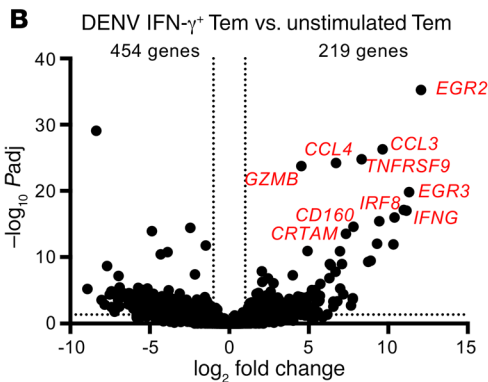
than their Tem counterpart. This effect was even more apparent when DENV IFN-γ+ Tem and Temra cells were examined, as 300 and 104 genes were upregulated in DENV IFN-γ+ Tem and Temra cells, respectively (Figure 2E), which resulted in an approximately 3-fold change and likely reflected antigen-driven differentiation resulting in selective expression of fewer genes.

Gene ontology (GO) annotations indicated that DE genes upregulated in DENV IFN-γ+ Tem and Temra cells by comparison with
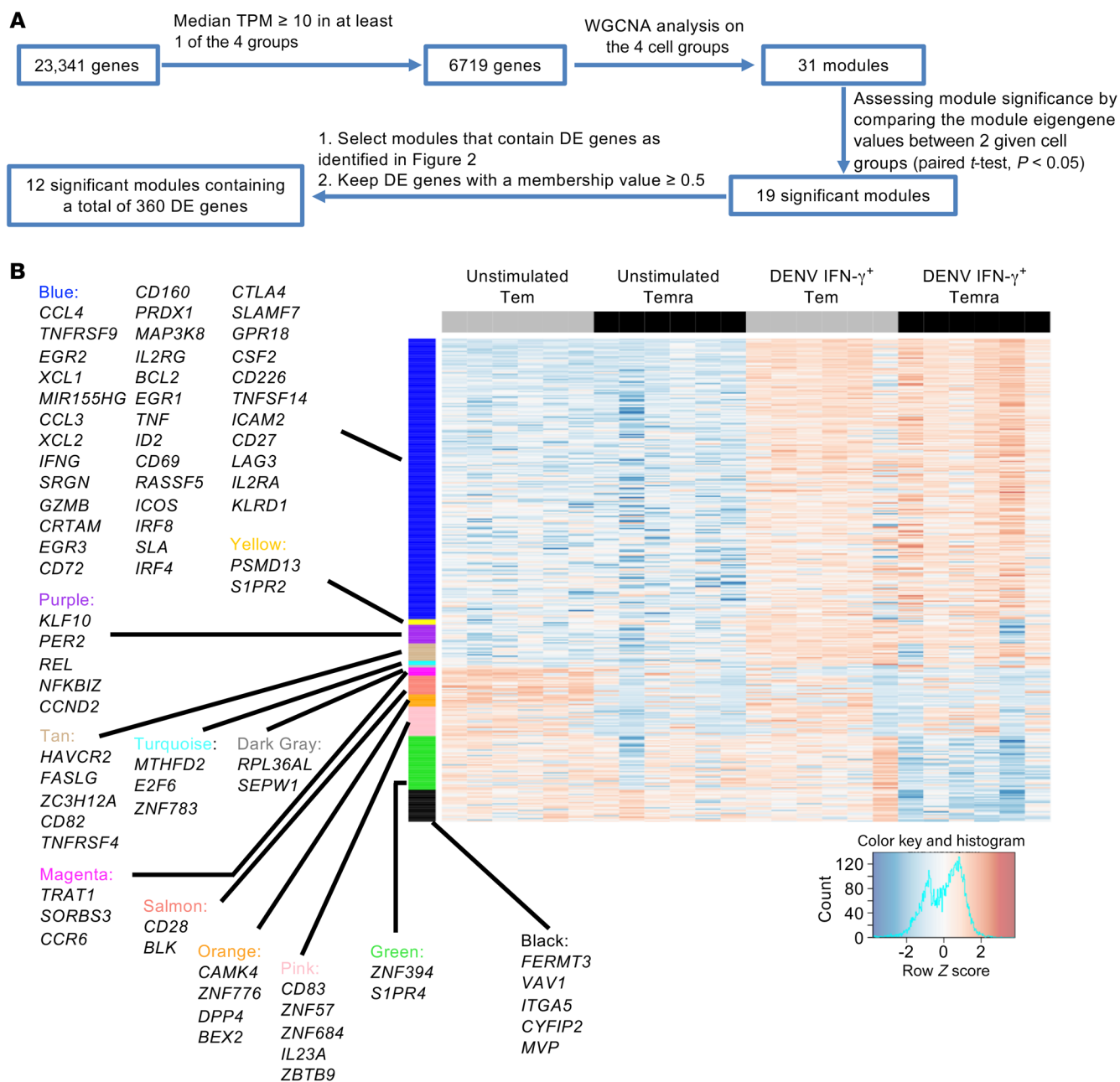
Figure 3. Identification of gene modules that can discriminate between unstimulated and DENV IFN-γ⁺ CD8⁺ Tem and Temra cells. (**A**) Schematic depicting the strategy for coexpression and clustering analysis. Module significance was assessed by comparison of the module eigengene values between DENV IFN-γ⁺ Tem and unstimulated Tem, DENV IFN-γ⁺ Temra and unstimulated Temra, unstimulated Tem and unstimulated Temra, and DENV IFN-γ⁺ Tem and DENV IFN-γ⁺ Temra cells. (**B**) Heatmap shows the Z-transformed expression values of the 360 differentially expressed (DE) genes contained by the 12 significant modules. Selected genes from each module are highlighted.

their unstimulated counterparts were associated with cytokine responses and metabolic processes (Supplemental Figure 3, A and B). DE genes upregulated in unstimulated Temra cells by comparison with unstimulated Tem cells were associated with immune response regulation and cellular defense (Supplemental Figure 3C). DE genes upregulated in unstimulated Tem cells by comparison with unstimulated Temra cells and DE genes between DENV IFN-γ⁺ Tem and Temra cells were not significantly associated with any GO terms.

For Figure 2, D and E, by applying a Venn diagram approach to the 85 and 104 genes upregulated in unstimulated Temra and

DENV IFN-γ⁺ Temra by comparison with unstimulated Tem and DENV IFN-γ⁺ Tem cells, respectively, we found that only 6 genes, including *KIR2DL3* and *KIR3DL1*, were shared by these 2 lists of DE genes. In contrast, 79 genes were found to be specific for unstimulated Temra cells, whereas 98 were specific for DENV-specific Temra cells (Figure 2F and Supplemental Table 4). Unstimulated Temra cells had higher expression of genes including *CCL3*, *GNLY*, *IFNG*, and *ZEB2* than unstimulated Tem cells, suggesting that CD8⁺ Temra cells may be more activated than Tem cells at baseline without stimulation. In contrast, DENV IFN-γ⁺ Temra

Table 1. *P* values for each gene module for each comparison and the number of genes within each gene module

	DENV IFN-γ⁺ Tem vs. unstimulated Tem	DENV IFN-γ⁺ Temra vs. unstimulated Temra	Unstimulated Tem vs. unstimulated Temra	DENV IFN-γ⁺ Tem vs. DENV IFN-γ⁺ Temra	No. of genes
Blue	0.000	0.001	0.035	0.118	209
Yellow	0.001	0.128	0.387	0.054	4
Purple	0.003	0.325	0.161	0.274	14
Tan	0.004	0.253	0.039	0.331	13
Turquoise	0.007	0.604	0.173	0.108	3
Dark gray	0.963	0.030	0.510	0.049	2
Magenta	0.001	0.012	0.018	0.158	6
Salmon	0.059	0.585	0.030	0.339	14
Orange	0.037	0.435	0.041	0.462	9
Pink	0.899	0.614	0.042	0.520	22
Green	0.770	0.313	0.305	0.032	40
Black	0.613	0.008	0.585	0.036	24

Statistical significance was determined by 2-tailed paired Student's *t* test.

cells did not have higher expression of these genes than DENV IFN-γ⁺ Tem cells but upregulated genes such as *IL2RG*, which is referred to as the common γ chain and is a cytokine receptor subunit shared by IL-2, IL-4, IL-7, IL-9, IL-15, and IL-21 receptors.

Identifying gene modules that can discriminate between different CD8⁺ T cell populations. The data presented above suggest that CD8⁺ Temra cells have a more focused and selective pattern of gene expression than their Tem counterpart; this finding is more pronounced in antigen-specific T cells. We reasoned that this might be reflective of the activation of specific gene modules, encompassing genes that are coordinately expressed in the different T cell subsets. Accordingly, to better understand the biological functions associated with those DE genes, we performed weighted gene coexpression network analysis (WGCNA) (37, 38). Figure 3A depicts the analytic strategy. Briefly, we filtered out low-expressed genes with a median transcripts per million (TPM) value of less than 10 in all of the 4 cell populations. We identified 12 gene modules that were associated with statistically significant differences in least 1 of the 4 pairwise comparisons. The associated *P* values and the number of genes in each module are listed in Table 1. These 12 gene modules contained a total of 360 DE genes, which are listed in Supplemental Table 5 and were visualized on a heatmap as shown in Figure 3B.

We observed that there were 7 and 4 gene modules that could significantly distinguish DENV IFN-γ⁺ Tem and Temra cells from their unstimulated counterparts, respectively, and that 2 clusters (blue and magenta) were significant in both comparisons (Table 1). The blue, yellow, purple, tan, turquoise, and dark gray modules mainly discriminate between unstimulated and DENV IFN-γ⁺ Tem and/or Temra cells and contained activation- and effector-associated genes such as *CCL4*, *TNFRSF9* (encodes CD137), *CCL3*, *IFNG*, *GZMB*, *CRTAM*, *TNF*, *LAG3*, *NFKBIZ*, and *HAVCR2* (encodes Tim-3). Additionally, several transcription factors such as *BCL2*, *ID2*, *IRF8*, and *IRF4* and genes involved in T cell migration such as *SLAMF7* and *S1PR2* were also found in these clusters.

We found that the blue, tan, magenta, salmon, orange, and pink modules were statistically distinct between unstimulated

Tem and Temra cells when these 2 populations were compared directly (Table 1). Notably, the salmon and pink modules were statistically significant only in this comparison and contained genes such as *CD28* and *CD83*, which are involved in T cell activation. In contrast, the gray, green, and black modules distinguished DENV IFN-γ⁺ Tem and Temra cells (Table 1), and DENV IFN-γ⁺ Temra cells largely downregulated the genes contained in the green and black modules (Figure 3B). Thus, stimulation with DENV epitopes changes the differences between responding CD8⁺ Tem and Temra cells. These data further emphasize that a crucial difference between CD8⁺ Tem and Temra cells is the degree of selectivity in the pattern of gene expression, especially following antigen-specific stimulation.

Validation of differentially expressed genes by CyTOF. To validate the mRNA expression signatures of unstimulated and DENV IFN-γ⁺ CD8⁺ Tem and Temra cells, we used an independent set of donors and performed cytometry by time-of-flight (CyTOF) analysis on selected DE genes that were contained in the gene modules identified in Figure 3 and for which antibodies were commercially available. Owing to limited antibody availability for the genes that could discriminate DENV IFN-γ⁺ Tem and Temra cells, most of the molecules analyzed in Figure 4 were upregulated in DENV IFN-γ⁺ Tem and Temra cells as compared with their unstimulated counterparts. Consistent with gene expression analysis, the protein expression patterns largely matched what we observed at the gene expression level. By comparison with their unstimulated counterparts, DENV IFN-γ⁺ Tem and Temra cells had higher expression of activation and effector molecules such as CCL3/CCL4 (the anti-CCL3 antibody used cross-reacts with CCL4), CD69, CRTAM, IFN-γ, and TNF-α, costimulatory molecules such as CLTA4, ICOS, and LIGHT (encoded by *TNFSF14*), transcription factors including IRF4 and IRF8, and signaling lymphocytic activation molecule family member 7 (SLAMF7), which is involved in lymphocyte activation, inhibition, differentiation, and adhesion (Figure 4). The protein expression level of KIR2DL3 detected by CyTOF was generally low (Figure 4). There was no significant difference between DENV IFN-γ⁺ Tem/Temra and unstimulated Tem/Temra cells in terms of their KIR2DL3 expression at the protein level, and we only observed a subtle but significant difference between DENV IFN-γ⁺ Temra and DENV IFN-γ⁺ Tem cells (Figure 4). Two-way ANOVA analyses confirmed the hypothesis that markers on the DENV IFN-γ⁺ subsets had higher protein expression compared with their unstimulated counterparts with a *P* value of 0.0013 and 0.0044 for Tem and Temra cells, respectively. The bar graphs in Figure 4 show the contribution of individual markers to this difference and indicate the *P* values specific to each marker (comparisons used the 2-tailed Wilcoxon test, not corrected for multiple comparisons in order
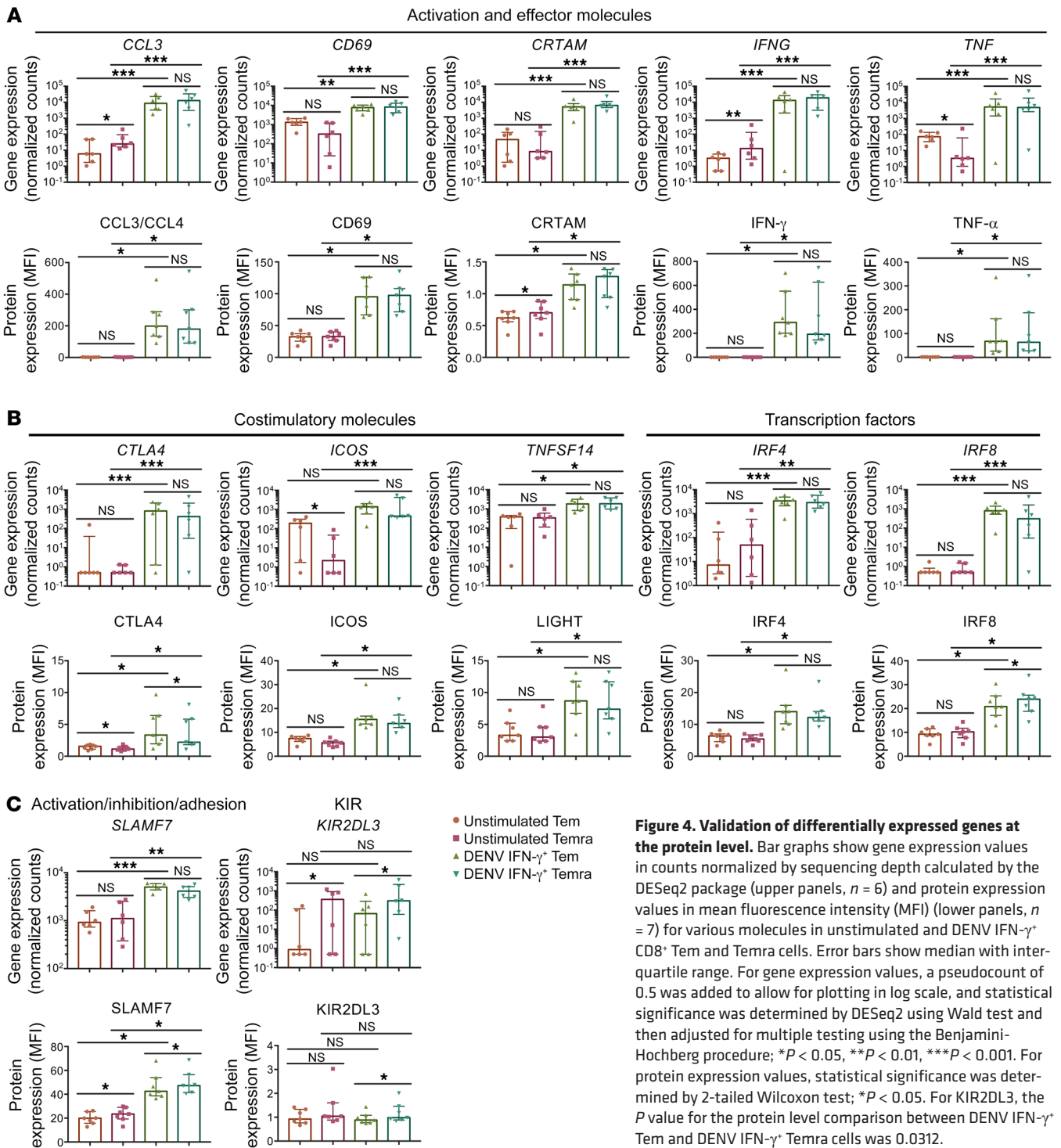
Figure 4. Validation of differentially expressed genes at the protein level. Bar graphs show gene expression values in counts normalized by sequencing depth calculated by the DESeq2 package (upper panels, $n = 6$) and protein expression values in mean fluorescence intensity (MFI) (lower panels, $n = 7$) for various molecules in unstimulated and DENV IFN-γ^+ CD8$^+$ Tem and Temra cells. Error bars show median with interquartile range. For gene expression values, a pseudocount of 0.5 was added to allow for plotting in log scale, and statistical significance was determined by DESeq2 using Wald test and then adjusted for multiple testing using the Benjamini-Hochberg procedure; *$P < 0.05$, **$P < 0.01$, ***$P < 0.001$. For protein expression values, statistical significance was determined by 2-tailed Wilcoxon test; *$P < 0.05$. For KIR2DL3, the P value for the protein level comparison between DENV IFN-γ^+ Tem and DENV IFN-γ^+ Temra cells was 0.0312.

to best show the contribution of different markers to the overall results). Based on Šidák's multiple-comparisons test, TNF-α, IFN-γ, and CCL3/CCL4 reached statistical significance with an adjusted P value of 0.0059, <0.0001, and <0.0001, respectively. Taken together, the signatures identified based on mRNA expression were largely also detectable at the protein level.

We next performed single-cell analysis of CyTOF data to investigate potentially interesting dynamics of unique CD8$^+$ T cell subsets. The expression levels of 32 surface and intracellular

molecules by CD8$^+$ T cells were measured simultaneously, and 2-dimensional maps of the resulting high-dimensional data were generated by visualization of stochastic neighbor embedding (viSNE) (39). While Tn cells were arranged largely in one area of the map, Tcm and especially Tem and Temra cells displayed a broader distribution and were grouped into several distinct islands, suggesting that these memory subsets were heterogeneous and could be further divided into dynamic subpopulations (Figure 5A). Notably, IFN-γ^+ DENV-specific CD8$^+$ T cells formed a
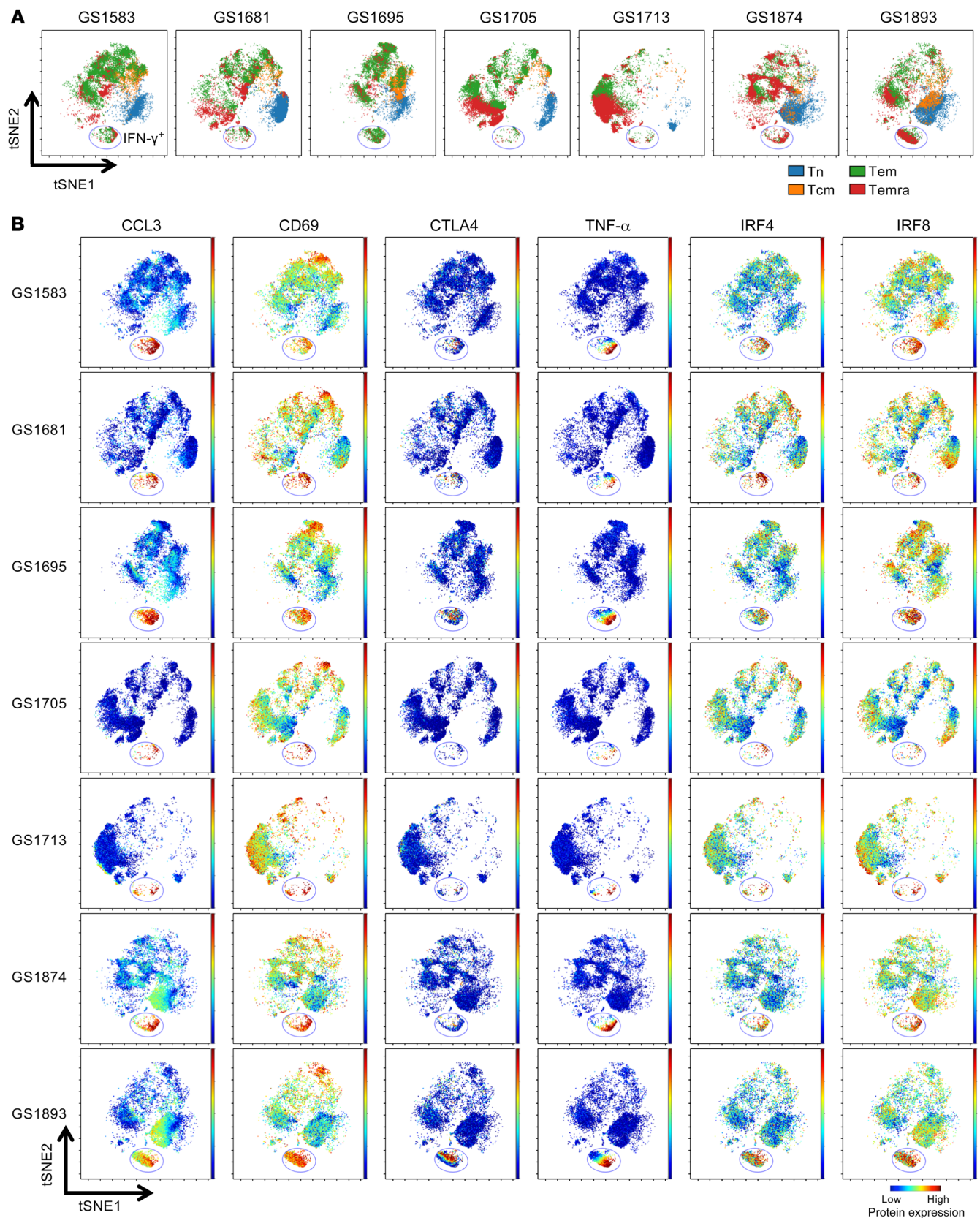
Figure 5. Single-cell analysis of high-dimensional CyTOF data reveals dynamics of CD8+ T cell subsets. viSNE analysis arranged cells along tSNE1 and tSNE2 axes based on the expression of 32 proteins (*n* = 7). (**A**) Manually gated Tn, Tcm, Tem, and Temra populations were colored and overlaid on the viSNE map of total CD8+ T cells for each donor. Gated population represented IFN-γ+ CD8+ T cells. (**B**) viSNE plots show the expression of CCL3, CD69, CTLA4, TNF-α, IRF4, and IRF8 per cell for each donor. Gated population represented IFN-γ+ CD8+ T cells.

distinct island and mainly consisted of Tem and/or Temra subsets with the relative proportion of these 2 subsets varying between donors (Figure 5A). Furthermore, within the island of IFN-γ+ cells, some molecules, such as CCL3 and CD69, showed clustered expression, while others, such as CTLA4, TNF-α, IRF4, and IRF8, displayed a gradient or mixture of expression (Figure 5B). Taken together, this approach revealed dynamic and intermediate states of CD8+ T cell activation.

DENV-specific Tem and Temra cells are associated with preferential TRBV gene usage. Previous studies show that CD4+ Temra cells with a cytotoxic phenotype have more restricted T cell receptor (TCR) repertoires compared with CD4+ Tem cells (33, 34). Based on these results and on the general gene expression patterns described above, we predicted that CD8+ Temra cells would also have a more restricted TCR repertoire than their Tem counterpart. To test this hypothesis, we next investigated whether unstimulated IFN-γ− as well as DENV IFN-γ+ CD8+ Tem and Temra cells also had distinct TCR repertoire characteristics. To this end, we extracted TCR β chain (TRB) CDR3 repertoires from the RNA-Seq data of sorted unstimulated IFN-γ− as well as DENV IFN-γ+ CD8+ Tem and Temra cells using MiXCR software (40, 41).

We observed that the TRB repertoire of unstimulated IFN-γ− CD8+ Temra cells is less diverse than that of unstimulated CD8+ Tem cells; however, this difference did not reach statistical significance (adjusted *P* value = 0.1014 with Dunn's multiple-comparisons test; Figure 6A). Likewise, there was a nonsignificant trend (adjusted *P* value = 0.1014 with Dunn's multiple-comparisons test; Figure 6A) for DENV-specific CD8+ Tem cells to have less diverse TRB repertoires compared with unstimulated Tem cells. The diversity of DENV IFN-γ+ Temra cells was similar to that of unstimulated Temra cells. Additionally, no significant difference was observed between DENV-specific CD8+ Tem and Temra cells (Figure 6A). The overall *P* value determined by Friedman test was 0.0228, and unstimulated Tem versus DENV IFN-γ+ Tem and unstimulated Tem versus unstimulated Temra were the 2 biggest contributors to this overall significance. Thus, these data may suggest that Tem cells may undergo clonal expansion in response to DENV antigens and that the Temra subset may mainly consist of highly clonally expanded cells.

We next evaluated the overlap of TRB repertoires by computing the normalized number of shared clonotypes using CDR3 amino acid sequences as previously described (42). This analysis revealed that the degree of overlap was higher between DENV-specific and unstimulated Temra cells compared with DENV IFN-γ+ and unstimulated Tem cells (Figure 6B). Nevertheless, the highest level of overlap was observed between DENV IFN-γ+ CD8+ Tem and Temra cells (Figure 6B), indicating that certain DENV CD8+ T cell epitopes are likely recognized by both Tem and Temra cells that share the same TCR.

Furthermore, we performed analysis of TRBV segment usage that revealed large variations between individual donors (Figure 6C and Supplemental Table 6), which was in line with the diverse MHC class I alleles of the cohort (Supplemental Table 1). Temra cells tend to have a narrower distribution in their TCR repertoires than Tem cells, as Temra cell TCR repertoires consisted of fewer segments than their Tem counterparts in 5 of the 6 tested donors (Figure 6C). Notably, in some donors DENV-specific CD8+ Tem

and Temra cells showed preferential usage of certain TRBV genes. For example, TRBV7-9 was expanded and overrepresented in both DENV-specific Tem and Temra cells in donor GS1149, whereas TRBV7-8 was predominantly used by DENV-specific CD8+ T cells, especially Tem cells, in donor GS1180 (Figure 6C). Intriguingly, in donor GS1188, TRBV9 was the single most predominant TRBV segment in DENV-specific Temra cells, whereas DENV-specific Tem cells were less biased, with TRBV4-3 being the most overrepresented TRBV segment in those cells (Figure 6C). Taken together, these data suggest that CD8+ Temra cells tend to have more biased TCR repertoires than Tem cells and that DENV-specific CD8+ Tem and Temra cells show both common and distinct TRBV gene usage in their TCR repertoires.

Discussion

This study is, to our knowledge, the first systematic analysis of isolated human virus-specific CD8+ memory T cell subsets, namely Tem and Temra cells. The current study built on previously published results implicating that CD8+ Tem and Temra cells are important in protection against viral pathogens and further characterized these CD8+ T cell subsets at the transcriptomic level, but it does not directly address protection. Our data show that the transcriptional profiles of antigen-specific CD8+ T cell subsets are highly different from those of unstimulated ones, thus highlighting the value of our approach and demonstrating that sequencing of bulk non–antigen-specific T cells alone will miss important determinants of the molecular programs. We further found that the differentiation of DENV-specific CD8+ T cell subsets, especially Temra cells, is associated with narrowing the transcriptional program and TCR repertoires program. The secondary donors studied here were from endemic areas and had been infected with DENV multiple times; therefore, it is expected that they had developed, at least to some extent, natural immunity from severe disease (43). These results could help guide the development of effective vaccines by providing a benchmark that vaccine-specific response could aim to replicate. According to the current study, a vaccine that elicits a strong CD8+ Temra response and specifically activates molecules such as CCL3/CCL4, CD69, CRTAM, IFN-γ, TNF-α, CTLA4, ICOS, LIGHT, IRF4, IRF8, SLAMF7, and KIR2DL3 would be expected to be of particular interest. Moreover, to our knowledge, this is the first transcriptomic profiling of isolated human antigen-specific CD8+ T cell subsets following stimulation with cognate antigen. The results have general implications for our understanding of the differentiation and activity of CD8+ T cell subsets.

The current study provides several insights into the gene expression profiles of unstimulated bulk versus DENV-specific CD8+ T cell subsets. Our data systematically characterized the immune signatures of DENV-specific CD8+ T cell subsets, and the expression of numerous genes was confirmed at the protein level by cytometry by time-of-flight (CyTOF). Collectively, the data indicate that CD8+ Temra cells have a more focused and selective gene expression pattern than Tem cells.

First, we showed that the majority of IFN-γ–producing CD8+ T cells in response to DENV epitopes display a Tem or Temra phenotype. Second, we identified genes that are upregulated in both DENV-specific Tem and Temra cell populations
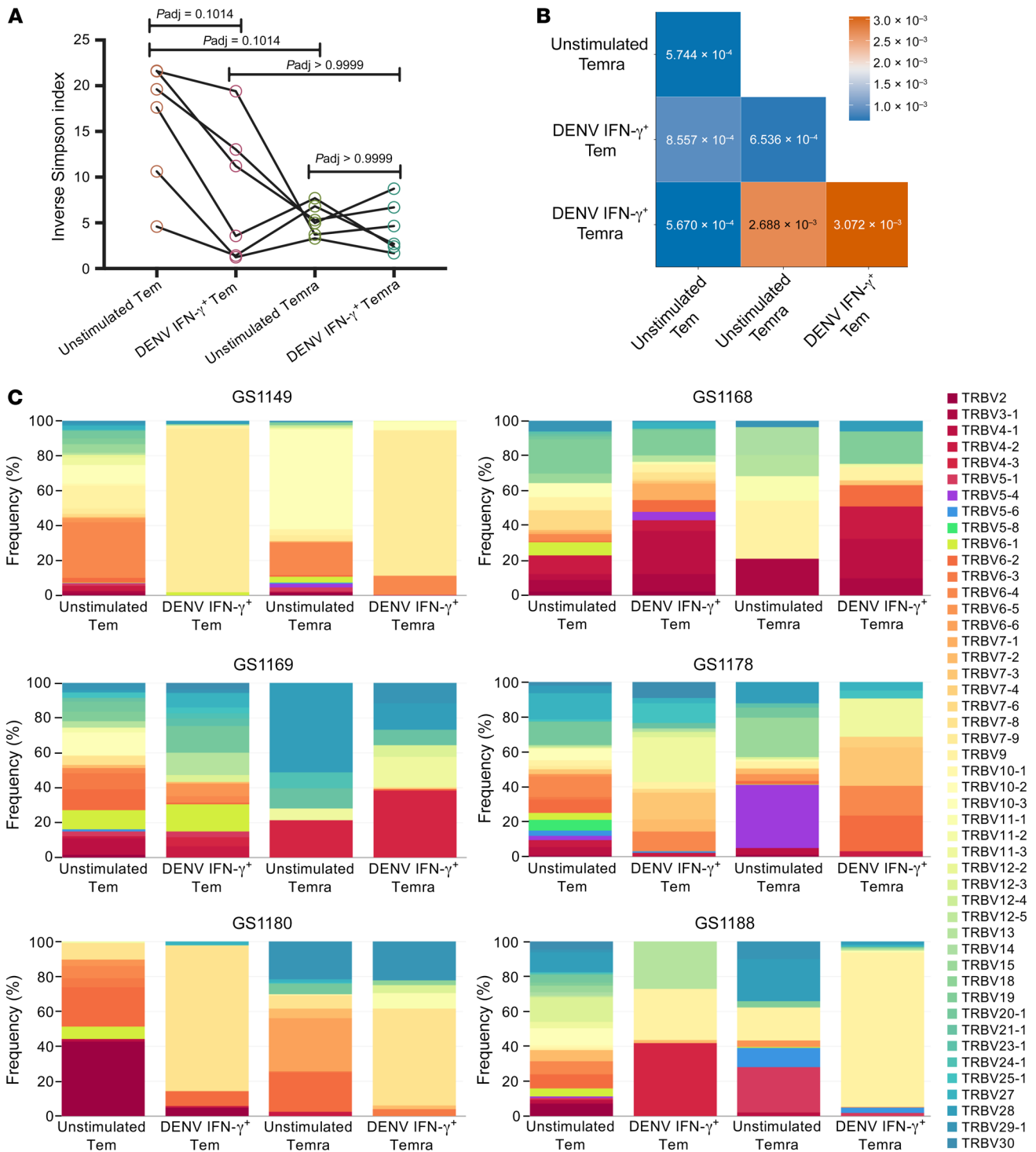
Figure 6. DENV-specific Tem and Temra cells have limited TCR repertoires and show preferential TRBV gene usage. (**A**) Dot plot shows the inverse Simpson index of the TCR repertoires of unstimulated and DENV IFN-γ[+] Tem and Temra cells ($n = 6$). Note that only 5 data points were discernible for the unstimulated Tem group, as 2 of the data points had almost identical values. The overall P value determined by nonparametric Friedman test was 0.0228. Statistical significance between groups was determined by Dunn's multiple-comparisons test, and adjusted P values are indicated in the figure. (**B**) Heatmap shows the normalized number of clonotypes with identical CDR3 amino acid sequences shared between CD8^{+} T cell subsets. (**C**) Bar graphs show the percentages of various TRBV segments within each population for each individual donor ($n = 6$).

following stimulation with DENV-specific epitopes, in comparison with their unstimulated counterparts. Coexpression and clustering analysis revealed gene modules that are upregulated in DENV-specific CD8^{+} Tem and Temra cells. These gene modules are associated with activation, costimulation, and effector functions, as they contain genes such as *CCL3*, *CCL4*, *CD69*, *CRTAM*, *CTLA4*, *ICOS*, *IFNG*, *IRF4*, *IRF8*, *SLAMF7*, *TNF*, and *TNFSF14*. Please note that our results do not point

to a single gene/factor that may determine the generation of CD8^{+} Tem or Temra cells. Additionally, the differentiation of CD8^{+} Tem and Temra cells is not unique to DENV infection, and we do not know whether the differentially expressed genes observed in the current study would also apply to other viruses. Third, we identified 2 sets of gene modules that distinguish Tem from Temra cells, one for unstimulated Tem and Temra cells, one for DENV-specific Tem and Temra cells. By comparing Tem and Temra cells directly, we found that more genes are expressed at higher levels in Tem cells than in Temra cells. In contrast, Temra cells have higher expression of several killer cell immunoglobulin-like receptors (KIRs), including *KIR2DL3*, suggesting that Temra cells have more specialized phenotype and function. Finally, we discovered that DENV-specific CD8^{+} Tem and Temra cells displayed preferential TRBV gene usage, indicating clonal expansion of certain T cell clones.

Previous studies by Chandele et al. show that HLA-DR^{+}CD38^{+} and HLA-DR^{-}CD38^{+} effector CD8^{+} T cell subsets expand during the acute febrile phase of DENV infection, and these effector CD8^{+} T cells, especially those that are HLA-DR^{+}CD38^{+}, are highly activated and upregulate genes associated with T cell activation, proliferation, cytotoxicity, and migration (27). In this study, we further isolated DENV-specific CD8^{+} T cells via their production of IFN-γ in response to a comprehensive pool of CD8^{+} T cell epitopes derived from DENV. Moreover, we identified and analyzed DENV-specific Tem and Temra cells separately. Although our samples were collected from secondary DENV-infected donors who were healthy at the time of sample collection, we found that DENV-specific CD8^{+} Tem and/or Temra cells still upregulated many of the genes reported by Chandele et al., such as *XCL1*, *GZMB*, *CTLA4*, *HAVCR2*, *LAG3*, and *CD160*, suggesting that DENV-specific CD8^{+} T cells may maintain an activated differentiated state even at convalescent stage in donors that have been infected with DENV multiple times. Thus, these cells may respond rapidly and exert effector functions on DENV reinfections.

It has been previously shown that CD4^{+} Temra cells are heterogeneous and that GPR56-expressing Temra subpopulations have a specialized gene expression program characterized by the upregulation of cytotoxic molecules (33, 34). Consistent with these previous findings on CD4^{+} Temra cells, this study shows that CD8^{+} Temra cells also display a more focused and specialized gene expression profile than Tem cells. Pairwise comparisons between unstimulated Tem and Temra cells as well as between DENV-specific Tem and Temra cells reveal that the number of genes upregulated in Tem cells is much greater than that upregulated in Temra cells. It is likely that many active genes gradually reduce expression in Temra cells as they progress toward a more specialized differentiation state. In line with this notion, we found that CD8^{+} Temra cells have enhanced expression of several KIRs at the mRNA level, which is consistent with a previous report (44). Although KIRs are primarily expressed on NK cells, terminally differentiated CD8^{+} T cells can acquire the expression of KIRs (45). Furthermore, most KIR-expressing CD8^{+} T cells display a limited KIR repertoire (45). Notably, the DENV-specific Temra cell population only upregulate 2 (*KIR2DL3* and *KIR3DL1*) of the 5 KIRs that are upregulated by their unstimulated counterpart, likely manifesting extensive antigen-driven clonal expan-

sion. Nevertheless, the expression of KIR2DL3 at the protein level measured by CyTOF, with the anti-KIR2DL3 used in this study, was generally low, and we only observed a subtle but significant different between DENV Temra and DENV Tem cells. We also note that a few donors displayed higher *KIR2DL3* gene expression levels than the other donors. Given the standard deviation of the mean for these 2 groups, the differential expression of KIR2DL3 at the mRNA level between unstimulated Tem and Temra cells, and between DENV-specific Tem and DENV-specific Temra cells, should be interpreted with caution. Additionally, the difference in protein expression level of KIR2DL3 between unstimulated Tem and Temra cells was not significant, which was inconsistent with the RNA-Seq data. While protein and RNA levels are in general correlated, there are also instances such as BCL-6 (46) in which there is a lack of concordance between mRNA and protein expression. Likewise, protein expression levels of KIR2DL3 between DENV-specific Temra and DENV-specific Tem cells are significantly different, but the difference is very subtle. For this reason, the difference in KIR2DL3 expression should also be interpreted with caution. Although KIRs have been implicated in dengue disease severity (47–49), whether the expression of KIRs on CD8^{+} T cells has any functional role in anti-DENV immunity warrants further investigation.

One distinctive aspect of this study is the integration of transcriptional and phenotypic profiling with TCR analysis. Our analysis of TRB repertoire overlap between CD8^{+} T cell subsets reveals that DENV-specific CD8^{+} Tem and Temra cells have the highest degree of overlap. Thus, it is possible that some DENV-specific Tem and Temra cells may share certain CDR3 sequences as previously observed for HCMV-specific CD4^{+} Tem and Temra cells (50). Since Temra cells also have a more specialized gene expression profile, we speculate that some Temra cells may derive from Tem cell clones and then undergo clonal expansion and differentiation. We further analyzed the usage of TRBV segments in individual donors and observed that DENV-specific CD8^{+} Tem and Temra cells have preferential usage of certain TRBV genes particularly in some of the donors. Because of the variation in MHC class I alleles between donors in the cohort, we did not observe a single TRBV segment that is overrepresented in 2 or more donors. Nevertheless, 2 TRBV7 subgroup members, TRBV7-9 and TRBV7-8, are preferentially used by DENV-specific Tem and Temra cells in donors GS1149 and GS1180, respectively, and the 2 donors share 2 MHC class I alleles, HLA-B*35:03 and HLA-C*04:01. A few TRBV segments, including TRBV11-2, TRBV9, and TRBV12-3/4, have been reported to be commonly represented in HLA-A*11:01–restricted CD8^{+} T cells that are specific for the nonstructural protein epitope NS3$_{133}$ variants derived from DENV1, DENV3, and DENV4 (51). Notably, TRBV9 was also overrepresented in DENV-specific Tem and, to a much larger extent, Temra cells in donor GS1188, who possessed the HLA-A*11:01 allele. Thus, this study extends previous findings and further reveals the similarities and differences between DENV-specific Tem and Temra subsets in terms of their TCR features.

As total DENV-specific IFN-γ^{+} CD8^{+} T cell subsets were sorted and analyzed in the current study, one cannot rule out the possibility that protection against DENV is mediated by a subpopulation(s) harboring a specific TCR(s) instead of being mediated

homogeneously by the entire DENV-specific IFN-γ+ CD8+ T cell populations. It would be interesting to investigate whether or not such subpopulations with a specific TCR would display a mainly Temra phenotype.

Our data showed that there was no significant difference between unstimulated Temra and DENV-specific Temra cells in terms of the diversity of their TCR repertoires. This might be partially due to the fact that the TCR repertoires of stimulated DENV-specific Temra cells might already be enriched in the unstimulated Temra population in those donors as they have been infected multiple times with DENV. While Temra cells might be an important component of the potent adaptive immune response against DENV, additional studies are needed to clarify the specific roles of this subset in protecting against DENV and address how this subset functionally compares with Tem cells during DENV infection. Clearly, the establishing of functional correlates of DENV-specific CD8+ T cell subsets is hampered by the fact that murine models of DENV infection are limited and that Temra cells are only defined in humans, not in mice. Additional insights would be provided by extensive investigation of the correlation between the activity of DENV-specific Tem and Temra cells during acute DENV infection and disease outcomes, which is beyond the scope of the current study.

One remaining issue is whether the magnitude of DENV-specific CD8+ T cell response correlates with neutralization antibody titers. Clearly, the number of data points in the current study is not suited to establish a meaningful correlation, but can be inspected for trends to be followed up in future studies. Although our study was not designed to address this question, based on the 6 donors used for RNA-Seq, we found that 3 of the 3 donors with a higher response magnitude (>0.3% IFN-γ+ CD8+ T cells in response to DENV epitopes) had a median neutralization antibody titer greater than 500. In contrast, only 1 of the 3 donors with a low response magnitude (<0.3% IFN-γ+ CD8+ T cells in response to DENV epitopes) had a median neutralization antibody titer greater than 500. Future studies are needed to investigate whether DENV-specific CD8+ T cell responses are correlated with neutralizing antibody responses.

In summary, our data show that the differentiation program of human DENV-specific CD8+ T cell subsets, especially Temra cells, while being activated and polyfunctional, is associated with narrow transcriptional responses and TCR repertoires, and thus a more focused and specialized approach. These findings reveal immune signatures of human DENV-specific CD8+ Tem and Temra subsets and may have broad implications for understanding the differentiation of antigen-specific CD8+ T cell subsets.

Methods

Human blood samples. Blood samples from healthy adult blood donors of both sexes between the ages of 18 and 65 were collected anonymously by the National Blood Center, Ministry of Health, Colombo, Sri Lanka, between 2010 and 2016 and processed at the Genetech Research Institute as previously described (52). The details of the donors used in this study are listed in Supplemental Table 1.

Serology. DENV seropositivity was determined by anti-DENV IgG ELISA as previously described (53). Seropositive donors who experienced multiple infections with more than one DENV serotype were determined by flow cytometry–based neutralization assay (54) and are referred to as secondary DENV infection donors.

IFN-γ capture assay and cell sorting for RNA-Seq. Human PBMCs were rested overnight at 37°C in RPMI 1640 medium (catalog RP-21, Omega Scientific Inc.) supplemented with 5% human serum (catalog 100-512, Gemini Bio-Products), 2 mM L-alanyl-L-glutamine (Gluta-MAX-I, catalog 35050061, Thermo Fisher Scientific), 100 U/ml penicillin, and 100 μg/ml streptomycin (catalog 400-109, Gemini Bio-Products) and subsequently stimulated with DENV megapool (CD8 MP) (1 μg/ml for individual peptides) or left unstimulated for 3 hours at 37°C. The generation of the CD8 MP was previously described (19). Briefly, the CD8 MP consisted of 268 epitopes that were selected to account for 90% of the IFN-γ response in both Sri Lankan and Nicaraguan cohorts (18, 19, 35). The 268 peptides were pooled, lyophilized, and resuspended (1 mg/ml for individual peptides) to form a master mix, which was then used for stimulation. IFN-γ–producing cells were labeled using an IFN-γ Secretion Assay – Detection Kit (catalog 130-054-202, Miltenyi Biotec) according to the manufacturer's instructions. Subsequently, PBMCs were stained with anti–human CD3, CD4, CD8, CD14, CD19, CD45RA, and CCR7 (see Supplemental Table 7 for antibody details). CD8+ IFN-γ- and IFN-γ+ naive (CD14-CD19-CD3+CD4-CD8+CD45RA+CCR7+), Tcm (CD14-CD19-CD3+CD4-CD8+CD45RA-CCR7+), Tem (CD14-CD19-CD3+CD4-CD8+CD45RA-CCR7-), and Temra (CD14-CD19-CD3+CD4-CD8+CD45RA+CCR7-) cells were sorted into 8 μl of lysis buffer consisting of Triton X-100 (Sigma-Aldrich), recombinant ribonuclease inhibitor (Takara), and dNTP mix (Thermo Fisher Scientific).

*HLA-B*35:01 tetramer staining.* The source of the tetramers used in this study and tetramer staining were described previously (19). Briefly, tetramers incorporating eight HLA-B*35:01–restricted DENV epitopes contained in the CD8 MP (HPGAGKTKRY, TPEGIIPTLF, LPVWLAYKVA, TPEGIIPALF, TPEGIIPSMF, VATTFVTPM, IANQATVLM, and FTMRHKKATY) were provided by the NIH Tetramer Core Facility. The 8 tetramers were pooled and used to stain PBMCs at a 1:50 dilution for 90 minutes at room temperature. Additional phenotypic markers were added into the mixture after 1 hour. Samples were then acquired using an LSR II flow cytometer (BD Biosciences) and analyzed using FlowJo (Tree Star).

Microscaled RNA-Seq. For each condition, 200 cells were collected at 4°C in 8 μl of lysis buffer composed by 0.2% Triton X-100, 2 U/μl of recombinant RNase inhibitor (Clontech/Takara), 5 mM dNTP mix (Life Technologies) in a 0.2-ml PCR tube (MAXYMum Recovery, Axygen). Right after sorting, tubes were vortexed at medium speed, spun for 5 minutes at more than 2000 g, and stored at –80°C until the completion of the whole set of samples. Four microliters of each sample was amplified following the Smart-seq2 protocol (55, 56). Briefly, mRNA was captured using poly-dT oligonucleotides and directly reverse-transcribed into full-length cDNA using the described template-switching oligonucleotide (55, 56). cDNA was amplified by PCR for 18 cycles and purified using AMPure XP magnetic beads (0.9:1 [vol/vol] ratio; Beckman Coulter). From this step, for each sample, 1 ng of cDNA was used to prepare a standard Nextera XT sequencing library (Nextera XT DNA library prep kit and index kits, Illumina). Barcoded Illumina sequencing libraries (Nextera, Illumina) were generated using an automated platform (Biomek FXP, Beckman Coulter). Both whole-transcriptome amplification and sequencing library preparations were performed in a 96-well format to reduce assay-to-assay

variability. Quality control steps were included to determine the optimal number of PCR preamplification cycles, and library fragment size. Samples that failed quality controls were eliminated from downstream steps. Libraries that passed strict quality controls were pooled at equimolar concentration, loaded, and sequenced on the Illumina Sequencing platform HiSeq 2500. Libraries were sequenced to obtain more than 8 million 50-bp single-end reads (HiSeq Rapid Run Cluster and SBS Kit v2, Illumina) mapping uniquely to mRNA reference, generating a total of about 204.3 million mapped reads (median of about 8.6 million filtered mapped reads per sample).

RNA-Seq analysis. The single-end reads that passed Illumina filters were filtered for reads aligning to transfer RNA, rRNA, adapter sequences, and spike-in controls. The reads were then aligned to UCSC hg19 reference genome using TopHat v1.4.1 (57). DUST scores were calculated with PRINSEQ Lite v0.20.3 (58), and low-complexity reads (DUST > 4) were removed from the BAM files. The alignment results were parsed via SAMtools (59) to generate SAM files. Read counts to each genomic feature were obtained with the htseq-count program (60) using the "union" option. After removal of absent features (zero counts in all samples), the raw counts were then imported to DESeq2 v1.16.1 to identify differentially expressed genes between groups (61). Paired DE analysis was performed using a multifactor design that includes the donor information as a term in the design formula in DESeq2, which accounts for differences between the donors. Wald test P values were adjusted for multiple testing using the Benjamini-Hochberg procedure (62), and genes with an adjusted P value less than 0.05 and a shrunken $\log_2$ fold change greater than 1 or less than –1 were considered significantly differentially expressed between groups.

Transcripts per kilobase million for a given gene$_i$ in a given sample was calculated as follows: $TPM_i = 10^6 \times (N_i / L_i) / [\Sigma_j (N_j / L_j)]$, where N_i is the number of reads for gene$_i$, L_i is the length of gene$_i$, and $\Sigma_j (N_j / L_j)$ is the sum of the rate of reads per kilobase for all the genes present in the sample. Genes with a median TPM value less than 10 in all of the 4 cell groups were excluded (63).

The Web tool Enrichr (http://amp.pharm.mssm.edu/Enrichr/) was used to perform gene ontology (GO) biological processes enrichment analysis (64, 65). Fisher exact test was used to assess the significance of the enrichment, and biological processes with an adjusted P value less than 0.05 were considered significant.

Coexpression and clustering analysis. Weighted gene coexpression network analysis (WGCNA) was performed to identify sets of genes that share a similar expression pattern (37, 38). Genes with a median TPM value less than 10 in all of the 4 cell groups were excluded from the WGCNA analysis (63). A total of 31 coexpression modules were identified by WGCNA. The gene expression profile of a module was summarized by module eigengene, which is defined as the principal component of the module (37, 38). To determine which modules could discriminate between 2 given cell groups, we compared the module eigengene values between samples from each of the 2 given cell groups. Since each donor contributed 1 sample to each of the cell groups, we performed a paired t test and considered a P value of ≤0.05 as statistically significant. To further enrich the selected modules with genes that have a high "discriminatory" power, only those genes identified in differential expression analyses were retained (for the cases in which the module achieved significance). In addition, only DE genes with high intramodular connectivity (membership ≥0.5) were included.

CyTOF. PBMCs were stimulated with DENV CD8+ T cell peptide pool (1 μg/ml for individual peptides) or left unstimulated in the presence of brefeldin A (GolgiPlug, BD Biosciences) for 6 hours. Subsequently, CD8+ T cells were isolated from the PBMCs using a human CD8+ T cell isolation kit (Miltenyi Biotec) according to the manufacturer's instructions. Isolated CD8+ T cells were then stained with the viability marker cisplatin followed by a surface antibody cocktail. Subsequently, cells were fixed in PBS with 2% paraformaldehyde overnight at 4°C. The following day, cells were stained with an intracellular/intranuclear antibody cocktail after fixation and permeabilization using the Foxp3/Transcription Factor Staining Buffer Set (eBioscience). Before sample acquisition, cellular DNA was labeled with Cell-ID Intercalator-Ir (Fluidigm). Samples were then acquired using a Helios mass cytometer (Fluidigm). Antibodies used in CyTOF are listed in Supplemental Table 8. Visualization of stochastic neighbor embedding (viSNE) analysis of CyTOF data was conducted using Cytobank (66).

TCR analysis. MiXCR v2.1.5 (40, 41) was used to extract TCR β chain CDR3 repertoires from RNA-Seq data of sorted T cell subsets. Subsequent TCR β chain diversity and repertoire overlap analyses were performed using the tcR R package v2.2.1.7 (67), and gene usage was analyzed using VDJtools v1.1.7 (68).

Data availability. The RNA-Seq data were deposited in the NCBI's Gene Expression Omnibus (GEO) database under the accession code GSE116957 and ImmPort under the study number SDY 888.

Statistics. Two-tailed Mann-Whitney (unpaired), Wilcoxon (paired), Friedman (paired), or 2-way ANOVA test was used to determine statistical significance between groups using Prism software (GraphPad). Šidák's and Dunn's multiple-comparisons tests were performed using Prism software. Statistical significance of gene modules was determined by 2-tailed paired Student's t test.

Study approval. The institutional review boards of both the La Jolla Institute for Immunology and the Medical Faculty, University of Colombo (serving as the NIH-approved Institutional Review Board for Genetech), approved all protocols described in this study. Please note that Sri Lankan blood samples were discarded buffy coats from routine blood donations at the National Blood Center and thus were exempt from human subject review as suggested by the institutional review boards.

Author contributions

YT designed and performed experiments, analyzed data, and wrote the manuscript. YT, MB, and JL performed computational analysis. GS, SL, and PV prepared RNA-Seq libraries and coordinated RNA sequencing. NDSG and ADD collected samples and provided clinical information. EJP and SAM coordinated and performed HLA typing. RDA and AG helped YT with experiments. YT, DW, BP, and AS designed and directed the study and critically edited the manuscript.

Acknowledgments

Address correspondence to: Alessandro Sette, La Jolla Institute for Immunology, 9420 Athena Circle, La Jolla, California 92037, USA. Phone: 858.752.6916; Email: alex@lji.org.

1. Bhatt S, et al. The global distribution and burden of dengue. *Nature*. 2013;496(7446):504–507.
2. Halstead SB. Pathogenesis of dengue: challenges to molecular biology. *Science*. 1988;239(4839):476–481.
3. Rothman AL. Immunity to dengue virus: a tale of original antigenic sin and tropical cytokine storms. *Nat Rev Immunol*. 2011;11(8):532–543.
4. Guzman MG, Alvarez M, Halstead SB. Secondary infection as a risk factor for dengue hemorrhagic fever/dengue shock syndrome: an historical perspective and role of antibody-dependent enhancement of infection. *Arch Virol*. 2013;158(7):1445–1459.
5. Katzelnick LC, et al. Antibody-dependent enhancement of severe dengue disease in humans. *Science*. 2017;358(6365):929–932.
6. Weiskopf D, Sette A. T-cell immunity to infection with dengue virus in humans. *Front Immunol*. 2014;5:93.
7. Tian Y, Sette A, Weiskopf D. Cytotoxic CD4 T cells: differentiation, function, and application to dengue virus infection. *Front Immunol*. 2016;7:531.
8. Ngono AE, Shresta S. Immune response to dengue and Zika. *Annu Rev Immunol*. 2018;36:279–308.
9. Yauch LE, et al. A protective role for dengue virus-specific CD8+ T cells. *J Immunol*. 2009;182(8):4865–4873.
10. Zompi S, Santich BH, Beatty PR, Harris E. Protection from secondary dengue virus infection in a mouse model reveals the role of serotype cross-reactive B and T cells. *J Immunol*. 2012;188(1):404–416.
11. Zellweger RM, Miller R, Eddy WE, White LJ, Johnston RE, Shresta S. Role of humoral versus cellular responses induced by a protective dengue vaccine candidate. *PLoS Pathog*. 2013;9(10):e1003723.
12. Prestwood TR, et al. Gamma interferon (IFN-γ) receptor restricts systemic dengue virus replication and prevents paralysis in IFN-α/β receptor-deficient mice. *J Virol*. 2012;86(23):12561–12570.
13. Elong Ngono A, et al. Protective role of cross-reactive CD8 T cells against Dengue virus infection. *EBioMedicine*. 2016;13:284–293.
14. Zellweger RM, Tang WW, Eddy WE, King K, Sanchez MC, Shresta S. CD8+ T cells can mediate short-term protection against heterotypic Dengue virus reinfection in mice. *J Virol*. 2015;89(12):6494–6505.
15. Zellweger RM, Eddy WE, Tang WW, Miller R, Shresta S. CD8+ T cells prevent antigen-induced antibody-dependent enhancement of dengue disease in mice. *J Immunol*. 2014;193(8):4117–4124.
16. Rivino L, et al. Virus-specific T lymphocytes home to the skin during natural dengue infection. *Sci Transl Med*. 2015;7(278):278ra35.
17. Hatch S, et al. Intracellular cytokine production by dengue virus-specific T cells correlates with subclinical secondary infection. *J Infect Dis*. 2011;203(9):1282–1291.
18. Weiskopf D, et al. Comprehensive analysis of dengue virus-specific responses supports an HLA-linked protective role for CD8+ T cells. *Proc Natl Acad Sci U S A*. 2013;110(22):E2046–E2053.
19. de Alwis R, et al. Immunodominant Dengue virus-specific CD8+ T cell responses are associated with a memory PD-1+ phenotype. *J Virol*. 2016;90(9):4771–4779.
20. Kaech SM, Cui W. Transcriptional control of effector and memory CD8+ T cell differentiation. *Nat Rev Immunol*. 2012;12(11):749–761.
21. Sallusto F, Geginat J, Lanzavecchia A. Central memory and effector memory T cell subsets: function, generation, and maintenance. *Annu Rev Immunol*. 2004;22:745–763.
22. Sallusto F, Lenig D, Förster R, Lipp M, Lanzavecchia A. Two subsets of memory T lymphocytes with distinct homing potentials and effector functions. *Nature*. 1999;401(6754):708–712.
23. Kwissa M, et al. Dengue virus infection induces expansion of a CD14(+)CD16(+) monocyte population that stimulates plasmablast differentiation. *Cell Host Microbe*. 2014;16(1):115–127.
24. Sun P, et al. Sequential waves of gene expression in patients with clinically defined dengue illnesses reveal subtle disease phases and predict disease severity. *PLoS Negl Trop Dis*. 2013;7(7):e2298.
25. Nascimento EJ, et al. Gene expression profiling during early acute febrile stage of dengue infection can predict the disease outcome. *PLoS One*. 2009;4(11):e7892.
26. Popper SJ, Gordon A, Liu M, Balmaseda A, Harris E, Relman DA. Temporal dynamics of the transcriptional response to dengue virus infection in Nicaraguan children. *PLoS Negl Trop Dis*. 2012;6(12):e1966.
27. Chandele A, et al. Characterization of human CD8 T cell responses in Dengue virus-infected patients from India. *J Virol*. 2016;90(24):11259–11278.
28. Northfield JW, et al. Human immunodeficiency virus type 1 (HIV-1)-specific CD8+ T(EMRA) cells in early infection are linked to control of HIV-1 viremia and predict the subsequent viral load set point. *J Virol*. 2007;81(11):5759–5765.
29. Lilleri D, Fornara C, Revello MG, Gerna G. Human cytomegalovirus-specific memory CD8+ and CD4+ T cell differentiation after primary infection. *J Infect Dis*. 2008;198(4):536–543.
30. Akondy RS, et al. The yellow fever virus vaccine induces a broad and polyfunctional human memory CD8+ T cell response. *J Immunol*. 2009;183(12):7919–7930.
31. Dunne PJ, et al. Epstein-Barr virus-specific CD8(+) T cells that re-express CD45RA are apoptosis-resistant memory cells that retain replicative potential. *Blood*. 2002;100(3):933–940.
32. Sridhar S, et al. Cellular immune correlates of protection against symptomatic pandemic influenza. *Nat Med*. 2013;19(10):1305–1312.
33. Tian Y, et al. Unique phenotypes and clonal expansions of human CD4 effector memory T cells re-expressing CD45RA. *Nat Commun*. 2017;8(1):1473.
34. Patil VS, et al. Precursors of human CD4+ cytotoxic T lymphocytes identified by single-cell transcriptome analysis. *Sci Immunol*. 2018;3(19):eaan8664.
35. Weiskopf D, et al. Human CD8+ T-cell responses against the 4 Dengue virus serotypes are associated with distinct patterns of protein targets. *J Infect Dis*. 2015;212(11):1743–1751.
36. Thielens A, Vivier E, Romagné F. NK cell MHC class I specific receptors (KIR): from biology to clinical intervention. *Curr Opin Immunol*. 2012;24(2):239–245.
37. Langfelder P, Horvath S. WGCNA: an R package for weighted correlation network analysis. *BMC Bioinformatics*. 2008;9:559.
38. Langfelder P, Horvath S. Fast R functions for robust correlations and hierarchical clustering. *J Stat Softw*. 2012;46(11):i11.
39. Amir el-AD, et al. viSNE enables visualization of high dimensional single-cell data and reveals phenotypic heterogeneity of leukemia. *Nat Biotechnol*. 2013;31(6):545–552.
40. Bolotin DA, et al. MiXCR: software for comprehensive adaptive immunity profiling. *Nat Methods*. 2015;12(5):380–381.
41. Bolotin DA, et al. Antigen receptor repertoire profiling from RNA-seq data. *Nat Biotechnol*. 2017;35(10):908–911.
42. Putintseva EV, et al. Mother and child T cell receptor repertoires: deep profiling study. *Front Immunol*. 2013;4:463.
43. Whitehead SS, Subbarao K. Which Dengue vaccine approach is the most promising, and should we be concerned about enhanced disease after vaccination? The risks of incomplete immunity to Dengue virus revealed by vaccination. *Cold Spring Harb Perspect Biol*. 2018;10(6):a028811.
44. Rodriguez RM, et al. Epigenetic networks regulate the transcriptional program in memory and terminally differentiated CD8+ T cells. *J Immunol*. 2017;198(2):937–949.
45. Björkström NK, et al. CD8 T cells express randomly selected KIRs with distinct specificities compared with NK cells. *Blood*. 2012;120(17):3455–3465.
46. Allman D, et al. BCL-6 expression during B-cell activation. *Blood*. 1996;87(12):5257–5268.
47. Beltrame LM, et al. Influence of KIR genes and their HLA ligands in susceptibility to dengue in a population from southern Brazil. *Tissue Antigens*. 2013;82(6):397–404.

48. Alagarasu K, Bachal RV, Shah PS, Cecilia D. Profile of killer cell immunoglobulin-like receptor and its human leucocyte antigen ligands in dengue-infected patients from Western India. *Int J Immunogenet*. 2015;42(6):432–438.

49. Townsley E, et al. Interaction of a dengue virus NS1-derived peptide with the inhibitory receptor KIR3DL1 on natural killer cells. *Clin Exp Immunol*. 2016;183(3):419–430.

50. Abana CO, et al. Cytomegalovirus (CMV) epitope-specific CD4⁺ T cells are inflated in HIV⁺ CMV⁺ subjects. *J Immunol*. 2017;199(9):3187–3201.

51. Culshaw A, et al. Germline bias dictates cross-serotype reactivity in a common dengue-virus-specific CD8⁺ T cell response. *Nat Immunol*. 2017;18(11):1228–1237.

52. Weiskopf D, et al. Dengue virus infection elicits highly polarized CX3CR1⁺ cytotoxic CD4⁺ T cells associated with protective immunity. *Proc Natl Acad Sci U S A*. 2015;112(31):E4256–E4263.

53. Kanakaratne N, et al. Severe dengue epidemics in Sri Lanka, 2003–2006. *Emerging Infect Dis*. 2009;15(2):192–199.

54. Kraus AA, Messer W, Haymore LB, de Silva AM. Comparison of plaque- and flow cytometry-based methods for measuring dengue virus neutralization. *J Clin Microbiol*. 2007;45(11):3777–3780.

55. Rosales SL, et al. A sensitive and integrated approach to profile messenger RNA from samples with low cell numbers. *Methods Mol Biol*. 2018;1799:275–301.

56. Picelli S, Faridani OR, Björklund AK, Winberg G, Sagasser S, Sandberg R. Full-length RNA-seq from single cells using Smart-seq2. *Nat Protoc*. 2014;9(1):171–181.

57. Trapnell C, Pachter L, Salzberg SL. TopHat: discovering splice junctions with RNA-Seq. *Bioinformatics*. 2009;25(9):1105–1111.

58. Schmieder R, Edwards R. Quality control and preprocessing of metagenomic datasets. *Bioinformatics*. 2011;27(6):863–864.

59. Li H, et al. The Sequence Alignment/Map format and SAMtools. *Bioinformatics*. 2009;25(16):2078–2079.

60. Anders S, Pyl PT, Huber W. HTSeq — a Python framework to work with high-throughput sequencing data. *Bioinformatics*. 2015;31(2):166–169.

61. Love MI, Huber W, Anders S. Moderated estimation of fold change and dispersion for RNA-seq data with DESeq2. *Genome Biol*. 2014;15(12):550.

62. Benjamini Y, Hochberg Y. Controlling the false discovery rate: a practical and powerful approach to multiple testing. *J R Stat Soc Series B Methodol*. 1995;57(1):289–300.

63. Srikumar S, et al. RNA-seq brings new insights to the intra-macrophage transcriptome of Salmonella Typhimurium. *PLoS Pathog*. 2015;11(11):e1005262.

64. Chen EY, et al. Enrichr: interactive and collaborative HTML5 gene list enrichment analysis tool. *BMC Bioinformatics*. 2013;14:128.

65. Kuleshov MV, et al. Enrichr: a comprehensive gene set enrichment analysis web server 2016 update. *Nucleic Acids Res*. 2016;44(W1):W90–W97.

66. Kotecha N, Krutzik PO, Irish JM. Web-based analysis and publication of flow cytometry experiments. *Curr Protoc Cytom*. 2010;Chapter 10:Unit10.17.

67. Nazarov VI, et al. tcR: an R package for T cell receptor repertoire advanced data analysis. *BMC Bioinformatics*. 2015;16:175.

68. Shugay M, et al. VDJtools: unifying post-analysis of T cell receptor repertoires. *PLoS Comput Biol*. 2015;11(11):e1004503.